Photon Ranging for Upstream ONU Activation Signaling in TWDM-PON

Photon Ranging for Upstream ONU Activation Signaling in TWDM-PON

Luca Bertignono, Valter Ferrero, *Member, IEEE*, Maurizio Valvo, and Roberto Gaudino, *Senior Member, IEEE*

(Top-Scored)

***Abstract*—This paper focuses on upstream signaling in TWDM-PON (one of the two systems specified in the new series of ITU-T G.989.x Recommendations for NG-PON2), for what concerns the discovery phase of a new ONU. The key idea is that a new ONU, that needs to be discovered by the OLT, would send a low bit rate signal that is set to a sufficiently low-power level to not affect significantly the upstream transmission performance of already active ONUs. We properly dimension the key physical layer parameters of this technique and demonstrate it experimentally. We named this proposal as "photon ranging" due to its ultralow-power transmission and we experimentally demonstrate its feasibility. As a "side effect" of this study, we had to deeply revise the power penalty generated by the optical interferometric crosstalk, the main impairment that impacts the proposed setup, obtaining new results that may be of interest also in areas not directly related to the specific framework of TWDM-PON.**

***Index Terms*—Interferometric crosstalk, optical networks, optical transmission.**

I. Introduction

THE standardization process of the newest generation of passive optical network (PON) systems is currently on-going in ITU-T, leading to the NG-PON2 series of Recommendations G.989.x ([1]–[4]). One of the two standardized transmission options is called Time and Wavelength Division Multiplexing PON (TWDM-PON [2]) and it introduces dense WDM for the first time in the PON arena, making use of up to 8 wavelengths per direction on a 100 GHz grid for the downstream, and on a grid from 50 to 200 GHz for the upstream. This "revolution" opens an unprecedented capacity for PON, allowing bit rates of up to 80 Gbps in the downstream (and likely 40 Gbps in a first phase using 4 wavelengths). It also poses completely new technological hurdles for PON, mainly related to the issue of controlling the used wavelengths with the typical accuracy required by a 100 GHz channel spacing. Currently, one of the most relevant issues is how to develop tunable lasers and tunable optical filters at the very low target price of ONU hardware [5], [6]. As a consequence, one of the possible options under consideration to reduce costs is the use of wavelength uncalibrated tunable lasers at the ONU side that would be remotely driven to the proper wavelength position by proper algorithms controlled by the OLT, as proposed for instance in [5]. Anyway, an important side-effect of this setup arises in the upstream transmission. A newly activating ONU inside an already active PON (i.e. when there are already active ONUs that are regularly transmitting), being initially wavelength uncalibrated and time un-synchronized, may send a signal that is spectrally superimposed to one of the already active ONUs, potentially causing severe outage events. We briefly remind here that in GPON and XG-PON the activation problem is solved by opening "quiet windows" in the upstream TDMA (Time Division Multiple Access) frame where the ONUs in the activation phase can send their discovery requests in response to a grant issued by the OLT. The extension of the quiet window mechanism to the TWDM-PON scenario with wavelength uncalibrated ONU transmitters would require the upstream quiet windows to be time synchronized over all wavelengths (i.e. over all channels of operation of the TWDM-PON system). This solution anyway would prevent the interesting option of completely independent TWDM channels, as required for example in a multi-operator environment to implement unbundling on a per wavelength base. This is why we propose a solution that does not require any time coordination among the different channels by implementing a proper signaling mechanism, as briefly mentioned in [7] in the section dedicated to the so-called Auxiliary Management and Control Channel (AMCC) for TWDM. This paper, extending our previous [12], focuses on this signaling mechanism, analyzing and experimentally demonstrating a solution that satisfies two main targets:

1) Avoid any modification to the already specified physical layer (PHY) of the TWDM-PON standard.
2) Minimize the power penalty on the already active ONUs (which we will indicate as the "Data" ONUs) during the discovery phase of a new ONU (which we indicate as "Control" ONU).

In our proposal, this is obtained by transmitting upstream AMCC signaling at a sufficiently low optical power level (this is why we named this proposal "photon ranging" technique) in order to have less than 0.3 dB power penalty on the data signals. The proposed idea is schematically represented in Fig. 1 (upper part, time domain representation): while the active ONUs regularly transmit in the upstream using the standard TDMA burst-mode approach, a "photon ranging" signal is generated by the activating new ONU at a power level that is sufficiently low

Manuscript received July 28, 2015; revised September 15, 2015; accepted September 15, 2015. Date of publication September 21, 2015; date of current version March 3, 2016. This work was supported by a research contract with Telecom Italia S.p.A., Milano, Italy.

L. Bertignono is with the Istituto Superiore Mario Boella, Torino 10129, Italy (e-mail: d037365@ismb.it).

V. Ferrero and R. Gaudino are with the Dipartimento di Elettronica e Telecomunicazioni, Politecnico di Torino, Torino 10129, Italy (e-mail: valter.ferrero@polito.it; gaudino@polito.it).

M. Valvo is with Telecom Italia, Turin 10129, Italy (e-mail: maurizio.valvo@telecomitalia.it).

Color versions of one or more of the figures in this paper are available online at http://ieeexplore.ieee.org.

Digital Object Identifier 10.1109/JLT.2015.2480962

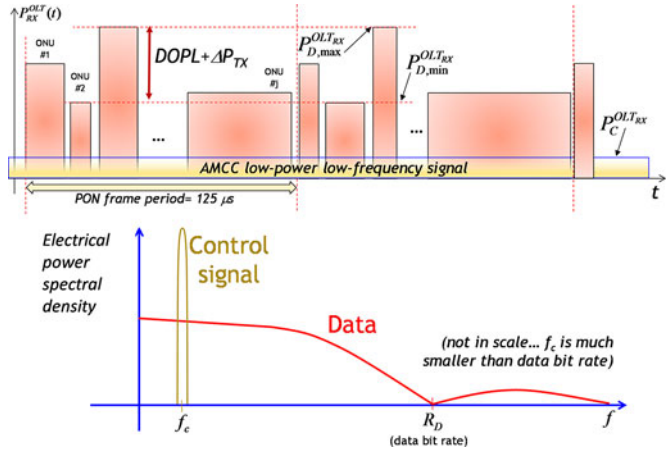

Fig. 1. Schematic representation of the power levels for the photon ranging proposal: in the time domain (top) and in the frequency domain after photo-detection (bottom).

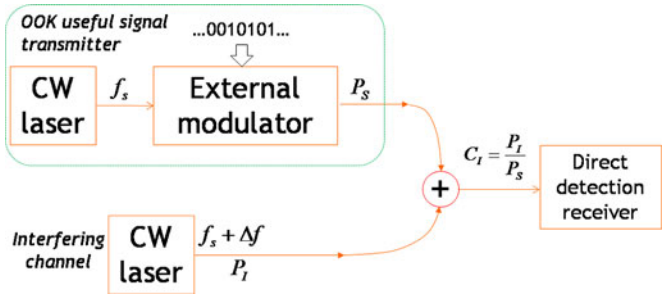

Fig. 2. Schematic block diagram of the system under test for the interferometric crosstalk evaluation under CW interfering signal.

to create negligible penalty on the active ONUs. Spectrally, after photo-detection, the situation is represented in the lower part of Fig. 1: the AMCC signal modulates a low-power and low-frequency subcarrier signal with a very low bit rate. Though it is received inside the data signal spectrum, the AMCC signal can spectrally "pop up" above the data spectrum (being its power concentrated in a very narrow spectral window) and, consequently, be detectable under proper conditions outlined in this paper. The acronyms used in Fig. 1 are: Differential Optical Path Loss (DOPL, up to 15 dB in the standard), ΔP_{TX} = difference in ONU output power (up to 5 dB), $P_{RX}^{OLT}(t)$power at the input of the OLT receiver, f_c = electrical frequency of the subcarrier.

The paper is organized as follows. In Sect. II, we review in detail (both theoretically and experimentally) the single-channel interferometric crosstalk effect that turned out to be a key issue in our proposal. In particular, we analyze a worst-case in which the low-power interfering optical signal is a continuous wave (CW) at exactly the same wavelength and polarization of the active high speed modulated signal, so to obtain a worst-case analysis of the crosstalk problem. In Sect. III, we experimentally extend these results to the case of low speed direct modulation on the interfering channel. The following Sect. IV is the core of our paper, since it presents the full system experiments of the photon ranging architecture, showing the feasibility of our proposal. In the final Sect. V we discuss our results, also introducing new system solutions.

II. Theoretical and Experimental Review of Single-Channel Interferometric Crosstalk Penalty

The key idea of our photon ranging signaling mechanism can be summarized as follows: in the upstream path of a TWDM-PON, an ONU that needs to be discovered will send, without receiving a specific grant from the OLT, a low power and low bit rate AMCC signal on an uncalibrated wavelength. Since this signal (which we will indicate in the following as the "*Control*" signal) may in general fall on the same wavelength of some of the already active ONUs (whose upstream signals will be indicated as "*Data*" signals), or very close to it, it could generate interference and thus a penalty on the data signal.

The goal of this Section (and of the following Sect. III) is to investigate on this penalty, which should be kept below extremely small values (such as fractions of dBs) if we want the photon ranging technique to be (almost) transparent with respect to the active data signals. In general, we should analyze the resulting interference penalty on data under worst case conditions, that correspond to having the data and control optical signals on exactly the same wavelength and optical polarization. This is a situation that is usually referred to in the literature as single-channel interferometric crosstalk, using the terminology introduced by ITU-T in G.Sup39 [8]. This well known effect, indicated by other authors also as "coherent crosstalk" [10] or "homodyne crosstalk" [11] takes place in a direct detection (DD) receiver when an interfering channel is spuriously added to a useful received signal, and their two optical central frequencies are separated by less than the direct detection receiver electrical bandwidth. This is such a common and well-known topic that most authors today simply rely on the ITU-T G.Sup39 formulas (9.31) and (9.32), that give a simple closed-form estimate for the resulting power penalty under the assumption of binary On-Off Keying (OOK), for the two cases of optimal or average threshold at the receiver. Surprisingly, when we applied these ITU-T estimations to our case, we found a great discrepancy with our experimental results. As we will show in this Section, it turned out that the two ITU-T formulas are highly pessimistic when applied to the case of systems characterized by a high target bit error rate (e.g. $BER \leq 10^{-3}$ when Forward Error Correction, FEC, is used as is common in modern systems), and low acceptable penalty (e.g. less than 0.5 dB on the useful signal). We give in this Section new graphs for the exact penalty, and we confirm our theoretical results by both numerical simulations and by experiments under different realistic conditions.

The ITU-T G.Sup39 formulas (9.31) and (9.32) estimate the single-interferer interferometric crosstalk penalty for the setup shown in Fig. 2, as a function of the following two parameters:

1) Ratio C_I between the CW power of the interfering signal P_I and the useful modulated power $P_S (C_I = P_I/P_S)$. In all the following analysis, P_S and P_I are considered to be average optical power levels (and not peak power levels) to be consistent with the ITU-T definitions.
2) Extinction ratio *r* of the OOK useful signal

3) The ITU-T G.Sup39 formulas assume that both signals are OOK modulated, while in the following we specialized to the case of a modulated "main signal" corrupted by a CW interferer. This difference is taken into account in the comparison.

The ITU-T formulas assume a DD receiver limited by electrical additive Gaussian noise, which is a typical condition for DD receivers based on a photodiode plus transimpedance amplifier (PIN+TIA) structure without any optical amplification. Moreover, in order to be in the "interferometric crosstalk" case, the difference between the two lasers central frequencies (which we will indicate as the parameter Δf in the following) must be well below the DD receiver electrical bandwidth. To avoid any misunderstanding when comparing our results with the existing literature on this topic, we point out that in this Section we considered an un-modulated interferer (see Fig. 2) over a modulated useful signal, while the extension to a (low-speed) modulated interferer will be addressed in the following Section III.

For an optimized threshold receiver (i.e. a receiver where the decision threshold is set to the point minimizing the BER), the ITU-T estimate for the penalty in dB is (G.Sup39 formula (9.32) [8]):

$$\text{Penalty}_{\text{dB}} = -10\log_{10}\left(1-2\left(\frac{(1+\sqrt{r})\sqrt{10^{\frac{C_I}{10}}(r+1)}}{r-1}\right)\right) \quad (1)$$

A similar closed form formula (G.Sup39 formula (9.31) [8]) is available also for an average threshold receiver case. These two ITU-T formulas have a particularly simple closed-form expression since they are deduced under an upper-bound approximation derived from the theory developed in [9] (referred to in the ITU-T Supplement as the [b-Legg] theory), which we briefly summarize here. Let's consider a useful received OOK signal with instantaneous power $P_S(t)$, average power P_S and extinction ratio *r*, and an interfering signal with average power P_I (assumed for simplicity to be CW). Let Δf and $\Delta\phi$ be the frequency and phase difference between the two optical signals. The resulting photo-detected signal is proportional to:

$$s_{RX}(t) = P_S(t) + P_I + 2\sqrt{P_S(t)P_I}\cos(2\pi\ \Delta f\ t + \phi(t)) \quad (2)$$

In the ITU-T formula, probably in order to obtain a closed form expression, the random process $\beta(t) = \cos(2\pi\ \Delta f\ t + \phi(t))$ is upper bounded to its worst-case values $\beta = -1$ when a "1" is received on the useful signal, and $\beta = +1$ when a "0" is received. The resulting two levels after the photodiode for a received "1" or "0" are respectively (indicating with $P_{S,1}$ and $P_{S,0}$ respectively the received power levels for "1" and "0"):

$$\begin{aligned} s_{RX,1} &= P_{S,1} + P_I - 2\sqrt{P_{S,1}P_I} \\ s_{RX,0} &= P_{S,0} + P_I + 2\sqrt{P_{S,0}P_I} \end{aligned} \quad (3)$$

The resulting opening on the eye diagram is proportional to the difference between these two values, and is given by the following Eq. (4):

$$s_{RX,1} - s_{RX,0} = P_{S,1} - P_{S,0} - 2\sqrt{P_{S,1}P_I} - 2\sqrt{P_{S,0}P_I} \quad (4)$$

The power penalty given in Eq. (1) follows directly from Eq. (4) after some tedious but simple algebraic passages to calculate the increase in average power P_S necessary to obtain the same eye opening of the ideal crosstalk-less situation (which would simply be equal to $P_{S,1} - P_{S,0}$). Physically, the aforementioned condition on the random process $\beta(t)$ means that the crosstalk term at the output of the DD receiver has the worst-case value that corresponds to the unrealistic situation in which the interfering optical signal is always constantly out of phase by 180 degrees compared to the useful signal when a "1" is transmitted, and is always constantly in-phase when a "0" is transmitted. This is clearly an extremely pessimistic assumption that has the important advantage of resulting in a compact expression for the final estimate in Eq. (1), but completely neglects the exact statistics of the interferometric term, i.e. the exact nature of the random process $\beta(t)$. On the contrary, the exact approach given in [9] does not have a closed form expression, since it requires a numerical integration to get the exact BER and consequently, the resulting power penalty. In fact, the exact BER for optimal decision threshold using our previous receiver assumptions and notations is given by Eq. (5) at the bottom of this page, where $f_\beta(x)$ is the probability density function of the random process $\beta(t)$ and P_{th} is the decision threshold (which should be optimized in order to obtain the minimum BER). Curiously, the text accompanying ITU-T G.Sup39 formulas (9.31) and (9.32) states that the formulas are obtained using [9] but doesn't point out that they are actually an unrealistic upper bound to the exact theory. This can result in unrealistic excessively conservative estimations in some situations, as we will point out in the following section.

$$BER = \min_{P_{th}}\left(\frac{1}{4}\cdot\int f_\beta(x)\cdot\left(erfc\left(\frac{P_{S,1}+2x\sqrt{P_{S,1}P_I}-P_{th}}{\sqrt{2\sigma_n}}\right) + erfc\left(\frac{P_{th}-P_{S,0}-2x\sqrt{P_{S,0}P_I}}{\sqrt{2\sigma_n}}\right)\right)dx\right) \quad (5)$$

A. Numerical Results

We have numerically evaluated the results deriving from Eq. (5), assuming that in $\beta(t) = \cos(2\pi\Delta f t + \phi(t))$ the argument of the cosine is uniformly distributed in [0, 2π], as it happens in any practical situation due to the random variation of the relative phase of the two involved lasers. This assumption leads to the following probability density function for the random variable β:

$$f_\beta(x) = \frac{1}{\pi}\frac{1}{\sqrt{1-x^2}} \quad (6)$$

We compared the exact results obtained using Eqs. (5) and (6) to the ITU-T G.Sup39 formulas for several system cases. Even though we do not show the mathematical details here for lack of space, we also evaluated the case of average threshold

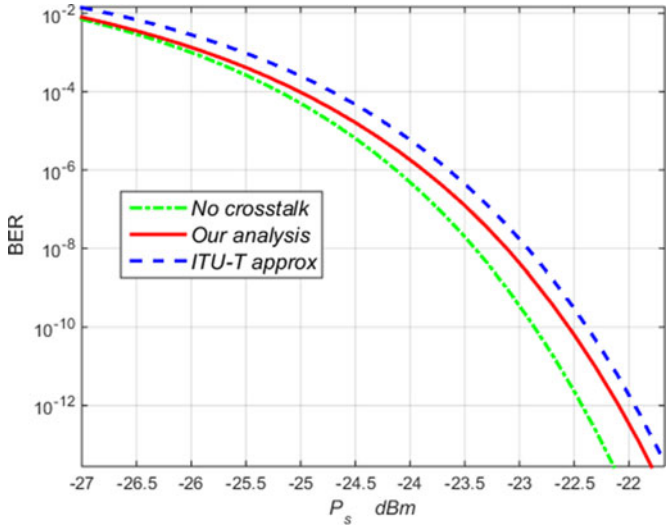

Fig. 3. BER as a function of the received power for $C_I = -25$ dB and Extinction Ratio equal to 13 dB for an optimal threshold receiver.

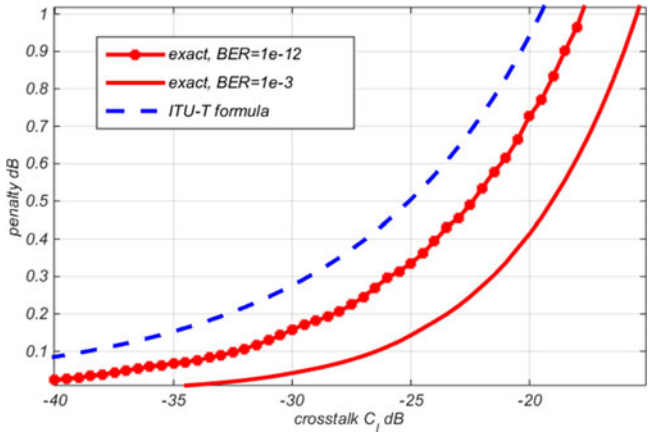

Fig. 4. Interferometric crosstalk power penalty in dB as a function of the crosstalk parameter C_I, optimal threshold receiver.

receiver. We start by showing in Fig. 3 the BER curves for a receiver that, in the absence of crosstalk, has a sensitivity of -26 dBm at $BER = 10^{-3}$ (close to the sensitivity of a class N1 2.5 Gbps NG-PON2 upstream receiver, for instance), for a high extinction ratio transmission ($r = 13$ dB) and a crosstalk level equal to $C_I = -25$ dB. In Fig. 3, we show the reference BER curve without crosstalk (dash-dot curve), the BER considering crosstalk and using the exact formula given by Eq. (5) (solid curve) and finally the one using the ITU-T approximation given by Eq. (1) (dashed curve). Alternatively, one can obtain the resulting power penalty at different BER levels as we have done in the following Fig. 4, which shows the penalty, as a function of C_I, estimated using the exact formula and the ITU-T approximation. This is done at two different target BER values, and in particular for $BER = 10^{-12}$ (the reference value for several optical transmission protocols that do not make use of FEC, such as the original version of most SONET/SDH systems) and then for a typical pre-FEC $BER = 10^{-3}$ (found e.g. in the most recent NG-PON2 standards for 10G transmission). We note from Fig. 4 that the ITU-T curve is pessimistic in all cases. For what concerns the photon ranging application in TWDM-PON, it is relevant that the discrepancy gets higher for higher BER, such as $BER = 10^{-3}$, while it is smaller for lower BER, such as for $BER = 10^{-12}$. This can somehow explain the ITU-T approximation: when the Supplement was originally released (more than 10 years ago), most systems were running at very low reference BER, since FEC was not used and, in this case, the ITU-T estimation is much closer to the exact value. An explanation of this behavior can be derived observing again the previous Fig. 3: the effect of crosstalk is more relevant for the (exact) BER curve when acting at low BER. Intuitively, this can be explained as follows: for a given signal power, the lower is the BER, the lower is the variance of the intrinsic receiver noise and, as a consequence, the relative impact of the crosstalk term becomes bigger. At high BER, the higher noise variance partially hides the relevance of the crosstalk term. The ITU-T approximation, being a worst case, predicts on the contrary a BER independent penalty, which is clearly not physical, and this also explains why the ITU-T approximation is less accurate at high BER, as shown in Fig. 4. As of today, most of the new optical transmission systems work at very high pre-FEC BER, where the ITU-T approximation really starts to be too pessimistic.

Just as an example, if one wants to design a system running at $BER = 10^{-3}$ and for which the acceptable interferometric crosstalk penalty is 0.2 dB, the ITU-T formula requires.

$C_I \leq -33$ dB, while the exact analysis leads to $C_I \leq -23.5$ dB. This example clearly shows that in an actual system design the ITU-T upper bound can lead to almost 10 dB unrealistic pessimistic estimation on the acceptable crosstalk level C_I.

As a further observation, both the ITU-T and exact formula consider a worst-case condition in which both the useful and the interfering signals are perfectly polarization aligned, while in almost any practical systems the two polarizations will be randomly oriented. In practice, this leads to a further decrease of the resulting penalty (we remind that in case of orthogonal polarization the penalty would be almost null).

In our analysis presented in Figs. 3 and 4, as already pointed out, we considered an un-modulated interferer (i.e. a CW optical signal), while the ITU-T formula considered an OOK signal also for the interferer. This difference was taken into account when deriving the ITU-T curve in Figs. 3 and 4. The following Fig. 5 shows the same types of curves for different values of extinction ratio (ER = 13 dB and ER = 6 dB), showing that the ITU-T approximation fits the trend of increasing penalty for decreasing ER values, but is again far from the exact value. For low extinction ratio (such as ER = 6 dB which is typical in several transmission systems) the 0.2 dB penalty is reached at $C_I \leq -27$ dB for the exact formula, and for $C_I \leq -37$ dB for the ITU-T approximation, again with approximately 10 dB unrealistic discrepancy. In general, for lower ER, the effect of interferometric crosstalk becomes higher because it gets relevant also on the logical "0" of the useful signal, since for decreasing ER the power on the "0" level becomes higher and thus "beats" more significantly with the interferer. On the contrary, for very high ER and thus for situation with almost no power on the "0" level, the effect of the interference is present only on the "1" level.

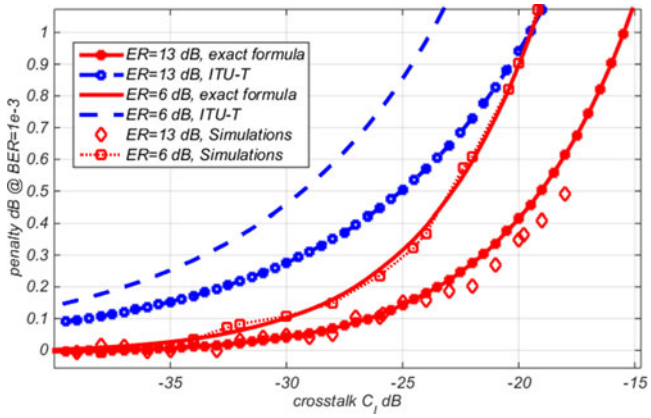

Fig. 5. Power penalty due to interferometric crosstalk using optimal threshold receiver, at $BER = 10^{-3}$.

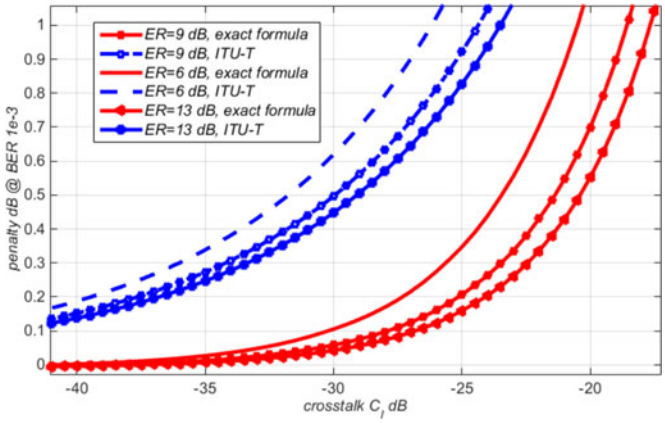

Fig. 6. Penalty for an average threshold receiver (for different ER values).

In the same Fig. 5, in order to check the validity of our exact evaluation, i.e. the theory developed in [9], leading to Eq. (5), we also superimpose the results obtained after a very detailed time-domain simulation. We performed a lengthy direct error-counting simulation (using the commercial optical system simulator OptSim) over more than 10^6 bits (to have reliable BER estimation around $BER = 10^{-3}$). The simulation results confirm the accuracy of the presented results.

Finally, we show in Fig. 6 the results for an average threshold receiver, i.e. a receiver for which the decision threshold is placed at the middle of the eye diagram, a typical solution implemented in low cost AC-coupled optoelectronic receivers. Once more, the inaccuracy of the ITU-T formula is quite evident also in this case.

B. Experimental Results

In order to get an experimental confirmation of our results, we also assembled an experiment in our lab where we replicate the same setup shown in Fig. 2. In order to be able to estimate penalties as low as 0.2 dB, we had to average our power and BER measurements over several hours (on every experimental curve). Moreover, to be in the same (worst case) condition of the previous Section, we used a polarization controller and a polarization analyzer to align the signal and interferer polarizations to a few degrees in the Stokes space. In order to ensure

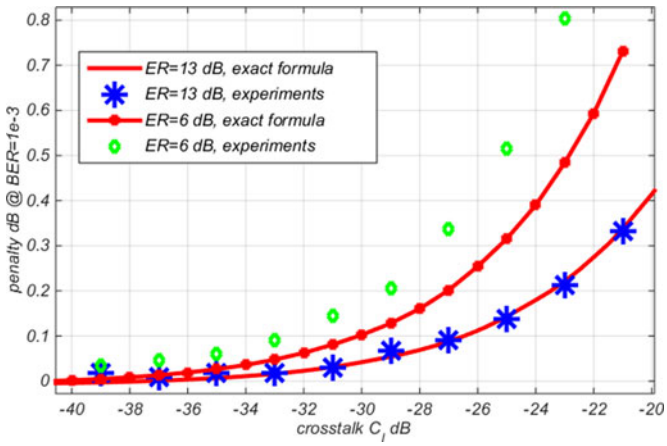

Fig. 7. Interferometric crosstalk power penalty in dB for different extinction ratio as a function of the crosstalk parameter C_I, optimal threshold receiver, $BER = 10^{-3}$: comparison between theory and experimental results.

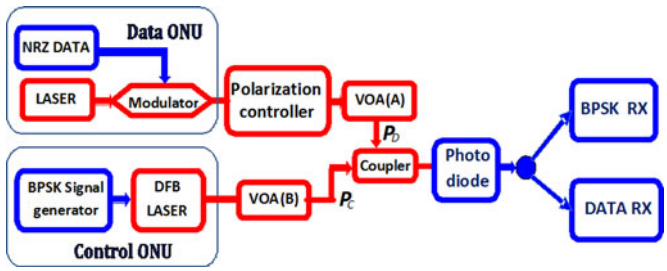

Fig. 8. Experimental setup. (VOA = Variable Optical Attenuator).

that the beating between the two signals was strictly inside the receiver electrical bandwidth, we also carefully aligned the two wavelengths during the measurements.

We show in Fig. 7 the experimental results for different ER (6 and 13 dB) comparing them to the exact theoretical curves. For the ER = 13 dB case, the agreement between theory and experiment is excellent, while there is a certain difference for the low ER case (ER = 6 dB). For instance, again for a 0.2 dB penalty the theory predicts $C_I \leq -27$ dB, while the experiments give $C_I \leq -29$ dB. This 2 dB difference is likely due to other second order effects that are not taken into account in the theory developed in [9], but again confirms also experimentally the inaccuracy of the ITU-T approximation, that in this case would give $C_I \leq -37$ dB.

III. Introducing Modulation on the Control Channel

In this Section, we present experimental results similar to the one obtained at the end of the previous section, but introducing a modulation on the interfering channel, using the setup shown in Fig. 8.

In view of the following Section, in which we will present full system experiments on the photon ranging architecture, we use here the same type of low-frequency modulation on the interfering optical signal that we will use for the control signal in the next section. This is a 2.5 MHz sinusoidal subcarrier signal on top of which a 2.5 kbit/s bit rate is applied using a 2-PSK electrical modulation; the resulting electrical signal is

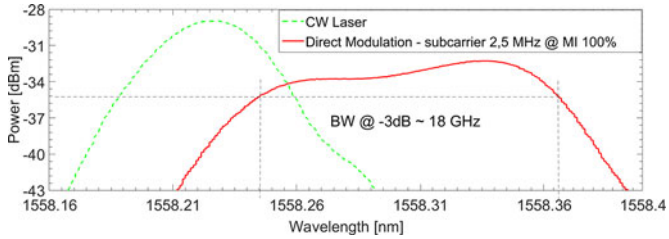

Fig. 9. Control ONU optical spectrum: green curve without control signal modulation, red curve with control signal direct modulation @ 2.5 MHz electrical subcarrier and modulation Index 100% (measurements by OSA with 0.1 nm Resolution Bandwidth).

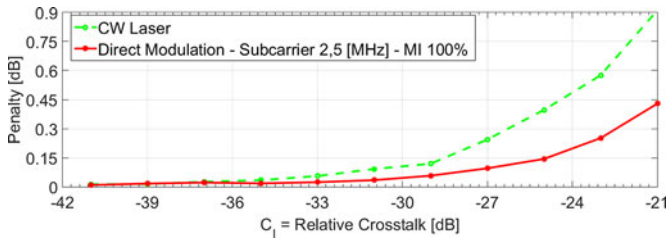

Fig. 10. Interferometric crosstalk penalty on the data signal (ER = 13 dB) with the wavelength alignment optimized and average threshold receiver: Green curve the control signal without modulation, red curve the control signal with direct modulation @ 2.5 MHz electrical subcarrier and modulation Index 100%.

applied to a directly modulated laser current input, to obtain a subcarrier amplitude modulation.

The control signal is electrically generated and applied to a directly modulated Fujitsu DFB commercial laser. The resulting optical spectra when the modulation is turned ON and OFF are shown in Fig. 9. For our following considerations, it is important to note that the direct modulated Control channel optical spectrum (red curve of Fig. 9) has a significantly larger optical spectrum compared to the CW case represented by the green curve of Fig. 9, due to thermal chirp effect in the directly modulated laser. In order to characterize the worst case interferometric crosstalk condition, we aligned the Data ONU ECL Laser wavelength and the control laser peak of the red curve of Fig. 9. The worst-case spectral alignment was searched by fixing a relative crosstalk of -19 dB and performing BER measurements for different Data ONU ECL wavelengths. We select the wavelength alignment that gave the worst-case BER.

The two variable optical attenuators (VOA A and B in Fig. 8) allow us to arbitrarily set P_C and P_D at the receiver (which was a commercial PIN+TIA receiver having a sensitivity at 2.5 Gbps equal to -25.95 dBm at $BER = 10^{-3}$ @ average threshold detection). Using these two VOAs we could thus also arbitrarily set the interferer-to-signal ratio $C_I = P_C/P_D$.

In order to evaluate with good repeatability the target very low level penalty on the received data power P_D *(fractions of dBs)*, we carry out several BER measurements versus the relative crosstalk C_I (20 repetitions), and perform averaging between them.

In the follow Fig. 10, we show the experimentally measured worst case interferometric crosstalk penalty on the data signal in the case of unmodulated Control signal (green curve), and

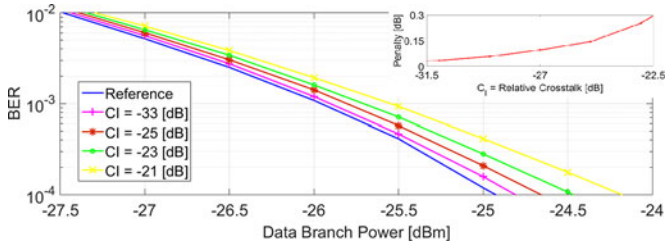

Fig. 11. BER on data for different relative crosstalk values C_I. The reference curve without the CONTROL channel is given in blue. The inset reports the resulting penalty @ $BER = 10^{-3}$.

in the case of modulated Control Signal (direct modulation of the laser by 2.5 MHz electrical subcarrier with 2.5 kbps BPSK), corresponding to the red curve. We observe that the penalty on the data channel is lower than the one shown in Figs. 3–6 presented in the previous Section. This is due to the fact that the low frequency direct modulation of the control laser does not only generate the (wanted) amplitude modulation but also a time-dependent optical frequency drift due to the laser chirp effects which typically extend to a few tens of GHz, as clearly shown in Fig. 9. As a result, the instantaneous optical frequency on the control signal is not always aligned to the central frequency of the Data signal (NRZ modulated at 2.5 Gbps) and, consequently, the "perfect" optical frequency alignment between the two signals that generates the interferometric crosstalk takes place only for a very limited fraction of time.

The resulting average crosstalk penalty is lower, which turns out to be a positive effect for the targets discussed in the following Section IV.

IV. Photon Ranging Full System Experiments

In this Section, using again the experimental setup shown in Fig. 8, we discuss the feasibility of our photon ranging proposal. We emulated two ONUs. The "Data" ONU generates a bit rate $B_D = 2.5$ Gbps NRZ signal (Extinction Ratio = 13 dB) using an external modulator. The "Control" ONU generates an electrical BPSK signal at a bit rate $B_C = 2.5$ kbit/s using a subcarrier at $f_{el,c} = 2.5$ MHz. The resulting electrical signal directly modulates a DFB laser. We looked for worst case conditions for what concerns interferometric crosstalk, by inserting a polarization controller that aligns the polarization of the two ONUs, and a temperature control on the DFB laser to have maximum optical frequency alignment between the two ONUs (i.e. the Data ONU and the Control ONU).

In Fig. 11, we show the BER curves for DATA at different crosstalk C_I, and the same is done for CONTROL in Fig. 12. In both cases, we also give reference curves without the respective interferers (in blue in the two graphs), to be able to estimate penalties compared to the reference situation, as it is shown for instance in the Fig. 11 inset in terms of penalty vs. C_I. The curves of BER on DATA (Fig. 11) clearly become worse for increasing C_I, and similarly in Fig. 12 the CONTROL shows worse BER performance for decreasing C_I. In fact, considering how we have defined the C_I, the DATA transmission would require low C_I, while the CONTROL transmission requires high C_I. After

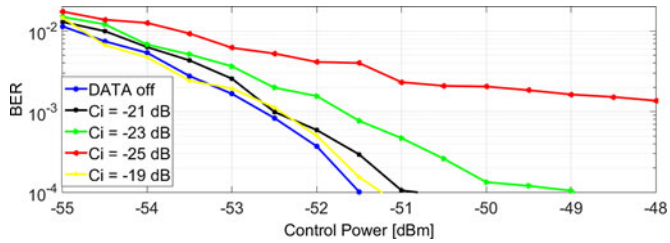

Fig. 12. BER on Control for different relative crosstalk values C_I. The curve without the DATA channel is also given as a reference.

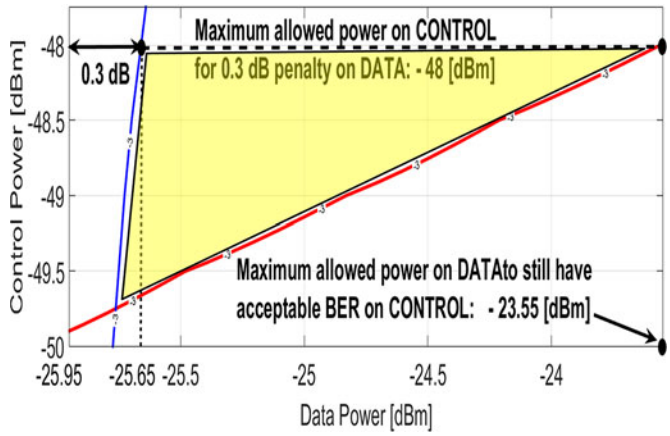

Fig. 13. Contour plot at $BER = 10^{-3}$ for data (purple curve) and control (red curve) in the a plane reporting P_C and P_D power levels.

these preliminary considerations, let us analyze more closely the actual numerical values. If we focus our attention at target $BER = 10^{-3}$, the penalty on DATA due to the simultaneous transmission remains below 0.3 dB up to a $C_I = -22.5$ dB, which is intentionally the highest C_I value that we show in the Fig. 11 inset. We interpret this result by saying that, if $C_I \leq -22.5$ dB, the simultaneous transmission of both control and data signals creates a negligible penalty on Data performance, even in the worst case of same wavelength and polarization. We then focus our attention on the control channel performance shown in Fig. 12. First, on the reference blue curve we observe that the -52.5 dBm control sensitivity value at $BER = 10^{-3}$ is much lower than the one for the data (-25.95 dBm), due to the much lower bit rate we need for the control (we have in our case that $B_C/B_D = 10^{-6}$). Moreover, it is also interesting to notice that the resulting penalty on control is very small up to $C_I = -22.5$ dB (between black and green curves), which means that the control is still detectable even when the data power is 22.5 dB higher than the control power. This apparently counterintuitive result is again due to the much lower bit rate. In fact, even though the total data power is very large compared to the control power, the fraction of data power that is present at the output of the narrow BPSK electrical receiving filter (of the order of 2 KHz bandwidth) is much smaller.

We show in Fig. 13 the contour plots at $BER = 10^{-3}$ for data (purple curve) and control (red curve) as a function of P_C and P_D. This is the most important and comprehensive result of our paper, but it requires a careful explanation to be properly understood. Let us define the point on the purple curve ($BER = 10^{-3}$ for data) that gives a 0.3 dB penalty on data performance, shown as the black dot in the upper left side of the picture.

This point sets the maximum value that P_C can assume, which turns out to be -48 dBm, since any value $P_C > -48$ dBm for the control power would give a penalty on data greater than 0.3 dB, which we set as our constraint for maximum acceptable penalty on data. Let us now focus on the control performance: this channel has acceptable performance (conventionally set to $BER_C < 10^{-3}$) in the area above the red curve given in Fig. 13. Thus, there is a region in the P_C and P_D plane in which both data and control work properly (i.e. the data has 0.3 dB penalty at most, and the control has $BER_C < 10^{-3}$). This region is approximately a triangle in the upper part of Fig. 13, highlighted in yellow and delimited by the purple curve, the red curve and the dashed line on the top.

As an important conclusion, assuming that the control power P_C is properly set, there is an operating region for P_D values ranging from the ideal (= no interference) sensitivity (-25.95 dBm) up to approximately -23.55 dBm, which we interpret as a "margin" on the allowed variation of P_D values of approximately 2.4 dB.

V. Discussion on Possible Evolution of Our Work

The results illustrated in Fig. 13 show that our "photon ranging" principle may work under proper power level conditions: a low power, low frequency control signal spectrally superimposed to a Data signal can be detected without creating significant power penalty on the Data signal itself. The operating range can be determined from Fig. 13 and shows that we have a few dBs of margin in terms of allowed variation of data power P_D. We honestly admit that the presented experiments do not yet satisfy the very demanding requirements set by ITU-T PON standards on power variation in the upstream. For instance, the differential optical path loss (DOPL) due to the ODN is specified by ITU-T to be up to 15 dB, while the ONUs transmitted power can have a 5 dB power variation allowance. These two specs give rise overall to a potential variation at the input of the OLT receiver of up to 20 dB among ONUs of the same PON tree (neglecting the additional contribution of the optical path loss) as graphically shown in upper part of Fig. 1. On the contrary, Fig. 13 shows that we have an available range for the data transmission received power P_D of up to 2.4 dB only. For higher data power, the control signal would not be detectable (i.e. $BER_C > 10^{-3}$). We are working on how to solve these issues, and we envision two possible solutions. A first solution would be the use of some power levelling mechanism (PLM) applied to all active ONUs transmitters, so that the received powers at the OLT are forced to be in a much smaller range than the aforementioned 20 dB. Even if PLM is being considered in the process of NG-PON2 standardization, for reasons completely independent on the AMCC photon ranging, as briefly mentioned for instance in [6] and [7], it is not expected to compensate for the entire power variation at the OLT receiver. However, we believe that the 2.4 dB margin shown in Fig. 13 can be improved in our

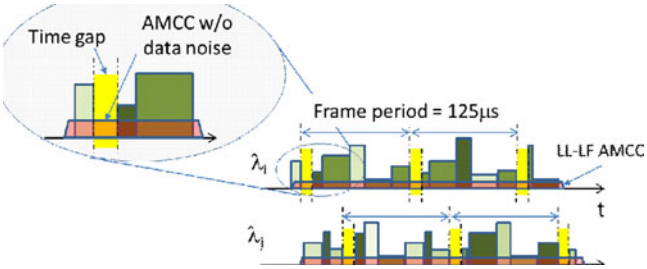

Fig. 14. Uncalibrated ONU discovery using the time-gap approach and a low-power low-frequency control signal AMCC.

forthcoming experiments through an optimization of the BPSK receiver (which for practical reasons we assembled in the lab using high frequency RF components, but could for sure be more performing using low-noise operational amplifiers more suited for the involved subcarrier frequency in the MHz range) and/or by relaxing some requirements. For instance, we have assumed a really small allowed penalty on data equal to only 0.3 dB, while setting it to, say, 0.5 dB would largely open the operating range.

As a second solution, we have envisioned a completely new approach, based on the following idea that we call the "time gap" approach, and schematically represented in Fig. 14. The data traffic of active ONUs is interrupted for short intervals of time (the "time gaps") in which the detection of the control signal would be much easier, since it is not interfered by any active data ONU. In particular, the control signal BER would be independent on DOPL values, simply because no active ONU is transmitting. Short upstream traffic interruptions can be easily achieved by transmitting unassigned grants. During the thus generated "time-gaps", samples of the AMCC signal can be acquired; time-gaps can be short enough to prevent disturbance to upstream traffic (excessive delay or jitter) and be repeated (for example once per frame) until acquisition of a full activation message, sent by the ONU attempting activation, is completed. Our preliminary calculations shows that these time gaps can be of the order of 1% of the upstream frame (which is set to 125 μs in all ITU-T PON standards). The absence of data generated noise during the time gaps makes the detection of the control signal much easier at the expense of a small fraction of upstream bandwidth. We also point out that synchronization among different TWDM channels is not required because the position of the time gaps can be completely asynchronous on each of the used wavelengths, that is independent operation of the different channels composing the TWDM system is possible.

In conclusion, though the results presented in this paper are only preliminary, we believe that our research work offers interesting hints on how AMCC can be implemented, for consideration and further discussion among the NG-PON2 community.

REFERENCES

[1] *40-Gigabit-capable passive optical network (NG PON2): Definitions, abbreviations and acronyms*, ITU-T Recommendation G.989, Mar. 2013.
[2] *40-Gigabit-capable passive optical networks (NG-PON2): General requirements*, ITU-T Recommendation G.989.1, Mar. 2013.
[3] *40-Gigabit-capable passive optical networks (NG PON2): Physical media dependent (PMD) layer specification*, ITU-T Recommendation G.989.2, Dec. 2014.
[4] *40-Gigabit-capable passive optical networks (NG PON2): Transmission Convergence Layer Specification*, ITU-T Recommendation G.989.3, Jul. 2015.
[5] N. Cheng and F. Effenberger, "Automatic ONU wavelength control in TWDM PONs," presented at the Opt. Fiber Commun. Conf. Exhib., San Francisco, CA, USA, Mar. 9–13, 2014.
[6] K. Grobe, M. H. Eiselt, S. Pachnicke, and J.-P. Elbers, "Access networks based on tunable lasers," *J. Lightw. Technol.*, vol. 32, no. 16, pp. 2815–2823, Aug. 2014.
[7] Y. Luo, M. Sui, and F. Effenberger, "Wavelength management in time and wavelength division multiplexed passive optical networks (TWDM-PONs)," presented at the IEEE Global Telecommun. Conf., Anaheim, CA, USA, 2012, pp. 2971–2976.
[8] *Optical System Design and Engineering Considerations*, ITU-T G.sup39 Recommendation, Sep. 2012.
[9] P. J. Legg, M. Tur, and I. Andonovic, "Solution paths to limit interferometric noise induced performance degradation in ASK/Direct detection lightwave networks," *J. Lightw. Technol.*, vol. 14, no. 9, pp. 1943–1954, Sep. 1996.
[10] R. Ramaswami, K. Sivarajan, and G. Sasaki, *Optical Networks: A Practical Perspective*, 3rd ed. San Mateo, CA, USA: Morgan Kaufmann, 2009.
[11] K. Ho, C. Chan, F. Tong, and L. K. Chen, "Exact analysis of homodyne crosstalk induced penalty in WDM networks," *IEEE Photon. Technol. Lett.*, vol. 10, no. 3, pp. 457–458, Mar. 1998.
[12] R. Gaudino, L. Bertignono, S. Capriata, V. Ferrero, L. Greborio, R. Mercinelli, and M. Valvo, "Photon ranging techniques for upstream signalling in TWDM-PON during ONU activation," presented at the IEEE Eur. Conf. Opt. Commun., Valencia, Spain, 2015.

Authors' biographies not available at the time of publication.